Journal of Geriatric Cardiology | JGC
RESEARCH ARTICLE
J Geriatr Cardiol 2024; 21(12): 1109–1118

Radiomics of baseline epicardial adipose tissue predicts left ventricular mass regression after transcatheter aortic valve replacement

Yi ZHANG[1,2], Hao-Ran YANG[1], Xing-Yu JI[1], Tian-Yuan XIONG[1,2,✉], Mao CHEN[1,2,✉]

1. Department of Cardiology, West China Hospital, Sichuan University, Chengdu, China; 2. Cardiac Structure and Function Research Key Laboratory of Sichuan Province, West China Hospital, Sichuan University, Chengdu, China
✉ Correspondence to: xiongtianyuan@wchscu.cn (XIONG TY); hmaochen@vip.sina.com(CHEN M)
https://doi.org/10.26599/1671-5411.2024.12.005

ABSTRACT

Background Epicardial adipose tissue (EAT) radiomics derived from cardiac computed tomography (CT) images may provide insights into EAT characteristics, which can further predict regression of left ventricular mass index (LVMI) after transcatheter aortic valve replacement (TAVR). This study aimed to develop and validate a radiomics nomogram based on pre-procedural EAT CT to predict inadequate LVMI regression following TAVR.

Methods Inadequate LVMI regression was defined as ΔLVMI% < 15% at one-year post TAVR. Radiomics features from pre-procedural CT images were selected mainly by least absolute shrinkage and selection operator algorithm. The patients were randomly divided into the training and validation cohorts to establish and evaluate three feature classifier models based on the selected features, using which the Radiomics scores (Radscores) were then calculated. A radiomics nomogram was constructed using independent risk factors and further assessed using area under the curve, calibration curve, and decision curve analysis.

Results A total of 144 consecutive TAVR patients (42 patients with inadequate and 102 patients with adequate LVMI regression) were randomly assigned to the training and validation cohorts (116 patients and 28 patients, respectively). A total of 1130 radiomics features from each patient yielded 6 features for the Radscore construction after selection, with logistic regression and support vector machine models favored. Subsequently, a nomogram based solely on the Radscore was constructed, with an area under the curve of 0.743 in the validation cohort, along with favorable decision curve analysis and calibration curves.

Conclusions The developed radiomics nomogram, serving as a non-invasive tool, achieved satisfactory preoperative prediction of inadequate LVMI regression in TAVR patients, thereby facilitating clinical management.

Left ventricular (LV) myocardial growth in patients with aortic stenosis (AS) is commonly observed as a compensatory response to increased LV afterload, a phenomenon known as LV remodeling. High LV mass was recognized as a robust predictor of all-cause mortality and morbidities in patients with or without AS.[1–3] Transcatheter aortic valve replacement (TAVR) has been shown to alleviate LV overload in AS patients, resulting in a rapid decrease in left ventricular mass index (LVMI) during the first year post-TAVR, with an average reduction of approximately 14.5%–22%.[4,5] Notably, greater LVMI regression at one year has been associated with lower rates of death and hospitalization up to five years.[4] Given its impact on prognosis, several predictors of inadequately reverse LV remodelling, such as male gender, TAVR-induced left bundle branch block, and a significant concomitant aortic regurgitation, have been proposed to guide clinical management.[5–7]

Apart from clinical characteristics, epicardial adipose tissue (EAT), an inflammatory visceral fat depot located within the pericardium, has been suggested to play a role in LV remodeling during the progression of calcific AS and in the clinical outcomes following TAVR.[8–10] Furthermore, the EAT computed tomography (CT)-radiomic and proteomic features have been found to be associated with adverse left atrial remodeling and post-operative atrial fibrillation (AF) in AS patient undergoing

aortic valve replacement.[11] These findings elucidate the potential role of EAT in cardiac remodeling, therefore we hypothesize that EAT radiomics may have the ability to predict LVMI regression. Considering preoperative CT imaging has become a routine assessment in contemporary TAVR practice, the utilization of EAT radiomics holds promise as a non-invasive approach to characterize EAT without additional cost.[12]

The objective of this study was to develop and independently validate a nomogram based on radiomics score (Radscore) for preoperative prediction of the probability of inadequate LVMI regression one year after TAVR in order to help identify high-risk patients and intervene early.

METHODS

Patient Information

The study involving humans were approved by Ethics Committee of West China Hospital (No.20191031), Sichuan University. All participants provided their written informed consent to participate in this study. This retrospective study included consecutive patients who underwent TAVR at our institution. The inclusion criteria were as follows: (1) patients with severe AS who met the indications for TAVR; (2) patients with complete medical and CT imaging records prior to TAVR; (3) patients who underwent successful bio-prosthesis implantation; and (4) patients with complete follow-up data of echocardiography at one year post-TAVR. The exclusion criteria were as follows: (1) patients who did not meet the indication for TAVR; (2) patients without complete medical records; (3) patients with incomplete image data and image artifacts; (4) patients without successful bio-prosthesis implantation; and (5) patients without complete 1-year follow-up. The TAVR procedure was performed according to routine protocols established in our center, as previously reported.[6] Sample size of this study was estimated based on one previous study with similar methodology.[13]

Baseline clinical features, including age, gender, body mass index (BMI), and comorbidities such as diabetes mellitus, hypertension, and AF, were collected. Additionally, baseline and 1-year transthoracic echocardiography were performed to assess LVMI. Measurements of left ventricular inner diameter in diastole (LVIDd), intraventricular septum in diastole (IVSd), and left ventricular posterior wall in diastole (LVPWd) were obtained using the parasternal long axis view, following guideline recommendations.[14] LVMI was calculated using the formula: LVMI = {0.8 × 1.04 × ([LVIDd + IVSd + LVPWd]^3 − LVIDd^3) + 0.6 g}/body surface area. Patients were divided into two groups based on the percentage change in LVMI (ΔLVMI%) (i.e., [baseline LVMI − 1-year LVMI]/baseline LVMI) at a threshold of 15%. This threshold was determined based on the reported average reduction of LVMI one year after TAVR. Patients with a ΔLVMI% ≥ 15% were classified as adequate LVMI regression and a ΔLVMI% < 15% as inadequate LVMI regression.[4,5]

CT Acquisition and Preprocessing

Pre-procedural cardiac CT scans were routinely conducted to facilitate procedural planning for TAVR. All CT scans were performed using a second-generation dual-source CT system (SIEMENS SOMATOM Definition Flash; SIEMENS Healthcare, Erlangen, Germany) and were contrast-enhanced. Manual delineation of pericardial borders was performed on axial images using the Horos software (version 2.0.2, Horos Project, Annapolis, MD, USA). The contours were delineated on multiple slices, starting from the level of the pulmonary trunk and ending at the level of the inferior diaphragmatic surface of the heart. The software automatically generated missing borders for other slices, which were manually adjusted as necessary. The region outside the traced pericardium was excluded, and the processed CT images were saved in DICOM format.

Extraction of Radiomics Features from EAT

The EAT was automatically segmented from the processed CT image using an open-source software, 3D Slicer (version 5.2.2, Slicer Community), with an attenuation range set between -10 and -190 Hounsfield Units. Subsequently, radiomics features of the EAT were extracted using an extension built upon the PyRadiomics package (version 3.0.1).[15,16]

Prior to the extraction of radiomics features, the CT images were resampled to an in-plane voxel size of 1 × 1 mm^3. For discretization of attenuations, a fixed bin width of twenty-five was selected. The radiomic features obtained from CT of EAT could be categorized into three main groups: (1) first order; (2) texture; and (3) shape features.[17] First order features were based on histograms and described the distribution of grey-level values for

EAT attenuation. Texture features, also known as second order features, characterized the spatial relationship between adjacent voxel attenuation values and quantify the heterogeneity and coarseness of adipose tissue using five matrices: grey-level co-occurrence matrix (GLCM), grey-level dependence matrix (GLDM), grey-level run-length matrix (GLRLM), grey-level size zone matrix (GLSZM), and neighborhood grey tone difference matrix (NGTDM). Shape features, including EAT volume, were intensity-independent features that describe the 3D geometric properties of EAT. After extraction from the original images, the first and second order features could be further enhanced using image filters such as Wavelet HHH, HHL, HLH, HLL, LHH, LHL, LLH, or LLL, and log sigma 1 mm, 2 mm, or 3 mm 3D. The shape features can be extracted solely from the original EAT images without the application of additional filters. The complete set of radiomics features extracted from the original EAT images was presented in supplemental material, Table 1S. To ensure the stability and reproducibility of the radiomic features, we evaluated inter-observer agreements in 20 selected cases across all feature groups.

Radiomics Features Selection

Three steps of feature selection were conducted. Firstly, intraclass correlation coefficients greater than 0.75 were utilized to guide the selection of stable features between radiomics features extracted from two groups of EAT regions drawn by two clinicians, both blinded to the LVMI regression outcomes when drawing EAT regions. Secondly, the *t*-test was applied to each stable feature between the inadequate and adequate LVMI regression cohorts, and features with *P*-values less than 0.05 were selected. Thirdly, the least absolute shrinkage and selection operator (LASSO) regression algorithm was employed to analyze and automatically select features through 5-fold cross-validation, based on the maximum area under the curve (AUC), with 100 repetitions to identify the most frequent and stable features.

Construction and Assessment of the Radiomics Nomogram

To validate the discriminative ability of the selected radiomics features for different LVMI regression modes, all patients were randomly divided into the training and validation cohorts at a ratio of 1:4. Three supervised machine learning algorithms, namely random forest, support vector machine, and logistic regression, were constructed using the selected features in the training cohort. Subsequently, these three algorithms were tested in the validation cohort. The performance of both the training and validation cohorts was evaluated using the AUC. Furthermore, the selected features with non-zero coefficients from the LASSO regression were used to calculate the Radscore for each patient. Finally, a radiomics nomogram based on the Radscore was established using logistic regression, after confounding analyze with factors including age, male sex, BMI, history of AF, aortic regurgitation degree more than mild, mean gradient of blood cross aortic valve. The predictive ability of the radiomics nomogram in both the training and validation cohorts was quantitatively measured using the AUC, and calibration curves.[18] To evaluate the clinical utility of the radiomics nomogram, decision curve analysis was performed by calculating the net benefits at different threshold probabilities for all patients.[19] The flowchart of this research is shown in Figure 1.

Statistical Analysis

Complete-case analysis was utilized for this study. Categorical variables were analyzed using Pearson's Chi-squared test, with Yates' correction or Fisher's exact probabilities applied when necessary. Continuous variables were analyzed using the Kruskal-Wallis rank sum test. A two-sided *P*-value < 0.05 was considered statistically significant. All data analyses were conducted using R software (v4.3.0, R Foundation for Statistical Computing).

RESULTS

Patient Information

A total of 144 consecutive patients undergoing TAVR were included in this study. One year post-TAVR, inadequate LVMI regression was observed in 42 patients (29.17%), while adequate LVMI regression was observed in 102 patients (70.83%). The demographic and clinical characteristics, as well as the Radscore, of patients in the training cohort, the validation cohort, and overall cohort are summarized in Table 1. There were no significant differences observed between the inadequate and adequate LVMI regression groups in terms of age, gender, BMI, the Society of Thoracic Surgeons predicted risk of mortality score, New York Heart Association class III-IV, and comorbidities including AF, hypertension,

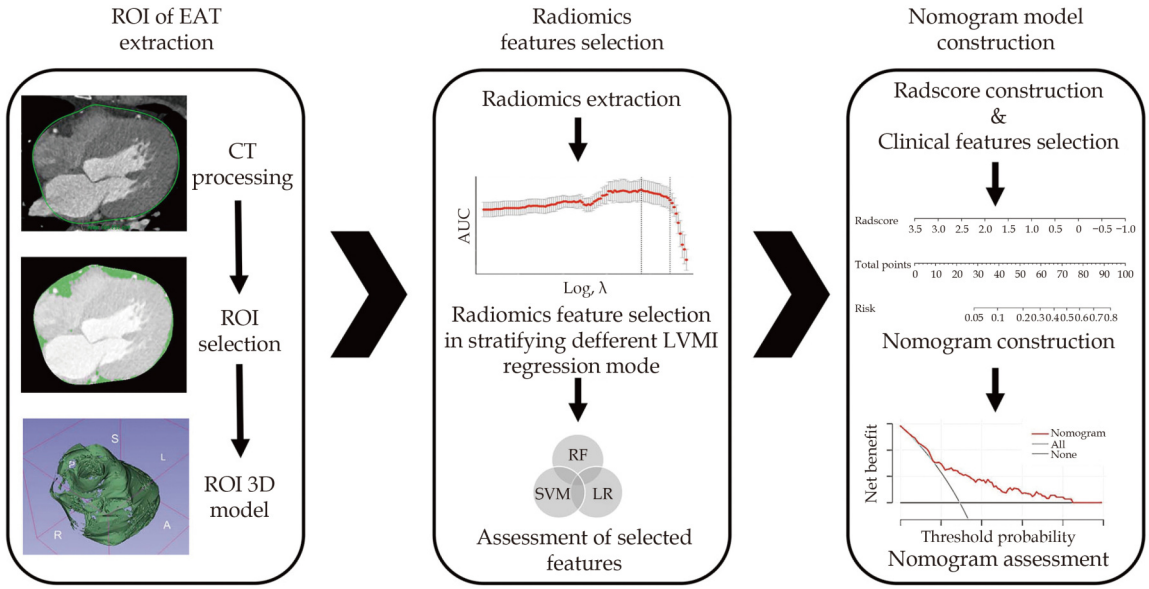

Figure 1 The flowchart of this study. CT: computed tomography; EAT: epicardial adipose tissue; LR: logistic regression; LVMI: left ventricular mass index; RF: random forest; SVM: support vector machine.

diabetes mellitus, coronary artery disease, echocardiographic parameters, and baseline EAT volume. However, the inadequate LVMI regression cohort exhibited significantly lower baseline LVMI ($P < 0.001$), and higher 1-year LVMI ($P < 0.001$).

Radiomics Feature Selection and Radscore Calculation

In this study, a total of 1130 radiomics features were extracted for each patient, encompassing 14 shape features, 18 first order statistics features, 75 texture features, 276 log sigma features, and 744 Wavelet features (supplemental material, Tables 1S & 2S). To ensure the reliability of the selected features, an initial screening was performed using the intraclass correlation coefficients, resulting in 838 stable radiomics features (supplemental material, Table 3S). Subsequently, a *t*-test was employed to further narrow down the feature set, resulting in the selection of 25 radiomics features. Finally, the optimal regulation weight λ (0.019583424), was determined for the best LASSO algorithm model. Then 6 features with non-zero coefficients were selected for stratification of different LVMI regression mode of TAVR patients. The detailed names and weights of the 6 radiomics features were shown in Figure 2.

Three supervised machine learning algorithms models were constructed to assess the ability of the selected radiomics features in discriminating different LVMI regression modes. The detailed performance of these models is presented in Table 2. The logistic regression and support vector machine models outperformed the random forest model. In the validation cohort, the logistic regression model achieved an AUC of 0.74, with sensitivity, specificity, accuracy, and F1 score values of 0.44, 1.00, 0.82, and 0.62, respectively. Similarly, the support vector machine model achieved an AUC of 0.74, with sensitivity, specificity, accuracy, and F1 score values of 0.22, 0.95, 0.71, and 0.33, respectively, in the validation cohort.

Subsequently, the Radscore for each patient in both the training and validation cohorts was calculated using coefficients of the best LASSO algorithm model. This calculation was performed using the following algorithm: Radscore = 0.43713186 × original-shape-maximum 2D diameter column + (−0.07561088) × log sigma 1 mm 3D-GLDM-dependence nonuniformity + 0.46241184 × log sigma 3 mm 3D-NGTDM-coarseness + 0.67098195 × wavelet HLL-firstorder-Kurtosis + (−0.22286110) × wavelet HLL-GLRLM-gray level variance + 0.11260365 × wavelet HLL-GLSZM-gray level variance + 1.00656474. Patients who exhibited inadequate LVMI regression demonstrated significantly lower Radscore values compared to patients with adequate LVMI regression ($P < 0.001$) (Figure 3). In the training cohort, the median Radscore values differed significantly between patients with inadequate LVMI regression and those with adequate LVMI regression (0.54 *vs.* 1.09, $P < 0.001$). A similar difference was observed in the validation cohort (0.27 *vs.* 1.25, $P < 0.001$).

Table 1 Characteristics of TAVR patients in the training cohort and validation cohort.

Variables	Training cohort (*n* = 116)			Validation cohort (*n* = 28)			Total cohort (*n* = 144)		
	Inadequate LVMI remodeling (*n* = 33)	Adequate LVMI remodeling (*n* = 83)	*P*-value	Inadequate LVMI remodeling (*n* = 9)	Adequate LVMI remodeling (*n* = 19)	*P*-value	Inadequate LVMI remodeling (*n* = 42)	Adequate LVMI remodeling (*n* = 102)	*P*-value
Age, yrs	74.00 (70.00–80.00)	73.00 (68.00–77.00)	0.15	74.00 (73.00–77.00)	75.0 (72.5–80.5)	0.81	74.00 (70.00–78.00)	73.50 (68.25–77.00)	0.21
Body mass index, kg/m^2	22.04 (20.03–23.88)	22.32 (20.20–24.70)	0.64	23.12 (22.31–24.22)	21.72 (20.98–23.25)	0.34	22.69 (20.26–24.01)	22.22 (20.31–24.57)	0.95
STS–PROM, %	6.25 (4.01–8.44)	6.65 (4.06–9.18)	0.56	5.89 (4.50–8.62)	7.79 (5.13–12.00)	0.57	6.07 (4.04–8.51)	6.73 (4.10–9.25)	0.46
NYHA III–IV	28 (84.85%)	73 (87.95%)	0.65	9 (100.00%)	18 (94.74%)	1.00	37 (88.10%)	91 (89.22%)	0.85
Atrial fibrillation	9 (27.27%)	10 (12.05%)	0.046	2 (22.22%)	4 (21.05%)	1.00	11 (26.19%)	14 (13.73%)	0.07
Hypertension	15 (45.45%)	31 (37.35%)	0.42	2 (22.22%)	8 (42.12%)	0.55	17 (40.48%)	39 (38.24%)	0.80
Diabetes mellitus	6 (18.18%)	13 (15.66%)	0.74	4 (44.44%)	4 (21.05%)	0.41	10 (23.81%)	17 (16.67%)	0.32
Coronary heart disease	14 (42.42%)	29 (34.94%)	0.45	3 (33.33%)	6 (31.58%)	1.00	17 (40.48%)	35 (34.31%)	0.48
Left ventricular ejection fraction, %	62.00 (55.00–69.00)	58.00 (42.50–68.00)	0.11	61.00 (42.00–64.00)	58.00 (46.00–67.00)	0.90	62.00 (55.00–69.00)	58.00 (43.00–68.00)	0.13
Maximum velocity of trans–aortic blood flow, m/s	4.70 (4.20–5.20)	5.10 (4.60–5.80)	0.02	5.00 (4.90–5.50)	4.80 (4.45–5.23)	0.43	4.85 (4.23–5.38)	5.03 (4.53–5.80)	0.06
Aortic regurgitation > mild	19 (57.58%)	55 (66.27%)	0.38	3 (33.33%)	15 (78.95%)	0.054	22 (52.38%)	70 (66.63%)	0.07
Mean pressure gradient of trans–aortic blood flow, mmHg	53.00 (47.00–65.00)	63.00 (51.00–83.00)	0.01	68.00 (63.00–71.00)	61.00 (48.50–69.00)	0.26	55.50 (47.00–70.25)	63.00 (51.00–82.00)	0.07
Epicardial adipose tissue volume, cm^3	118.98 (90.76–147.75)	104.20 (79.92–138.51)	0.26	105.77 (100.24–120.99)	78.29 (57.46–135.02)	0.21	116.15 (90.89–146.10)	103.40 (73.05–138.63)	0.14
Radscore	0.54 (–0.02–0.87)	1.09 (0.74–1.80)	< 0.001	0.27 (–0.18–1.44)	1.25 (0.69–1.81)	0.04	0.45 (–0.03–0.94)	1.20 (0.74–1.80)	< 0.001
Baseline LVMI, g/m^2	124.85 (109.57–159.99)	174.81 (144.20–211.23)	< 0.001	131.19 (112.15–141.30)	174.37 (144.93–201.85)	0.02	125.42 (110.44–158.12)	174.59 (144.20–210.43)	< 0.001
1–year LVMI, g/m^2	132.98 (112.10–152.11)	115.70 (99.48–135.61)	0.03	119.43 (108.84–128.13)	113.55 (101.78–140.93)	0.52	129.07 (111.46–151.79)	115.61 (99.84–138.50)	0.03
ΔLVMI%, %	–1.69 (–6.70–6.33)	–31.14 (–39.53––21.65)	< 0.001	–11.31 (–12.53––2.96)	–34.02 (–38.61––23.12)	< 0.001	–2.84 (–10.72–5.89)	–31.28 (–39.47––22.22)	< 0.001

Data are presented as *n* (%) or median (interquartile range). LVMI: left ventricular mass index; TAVR: transcatheter aortic valve replacement.

Establishment and Evaluation of the Radiomics Nomogram

In order to establish the radiomics nomogram, logistic regression analysis was performed using Radscore and clinical features to identify independent predictors of inadequate LVMI regression after TAVR. Univariate and multivariable logistic regression analyses were conducted. The result of the logistic regression analysis was presented in Table 3, indicating that only Radscore was a significant independent predictor of inadequate LVMI regression after TAVR.

Subsequently, a radiomics nomogram was constructed based on logistic regression analysis using only Radscore (Figure 4). The efficacy of the nomogram in assessing the probability of inadequate LVMI regression was evaluated using receiver operating characteristic curves. The AUC values for the training and validation cohorts were 0.765 and 0.743, respectively, demonstrating favorable sensitivity and specificity (Figure 5). The calibration curves of the proposed nomogram showed favorable outcomes in terms of the unreliability test, receiver oper-

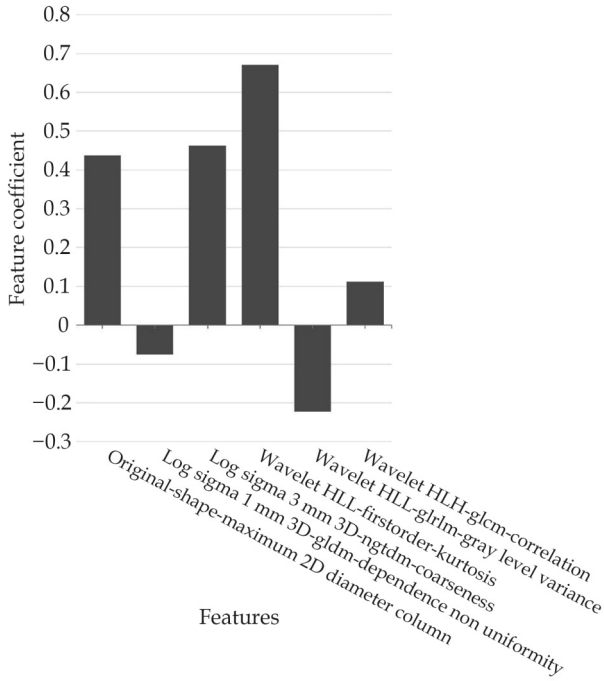

Figure 2 The weights of EAT radiomics features selected. EAT: epicardial adipose tissue.

ating characteristic area, slope, and bier index in both the training and validation cohorts (Figure 6). Furthermore, decision curve analysis demonstrated that the nomogram for predicting inadequate LVMI regression after TAVR could provide clinical net benefits (supplemental material, Figure 1S).

DISCUSSION

In this study, we firstly developed and validated the Radscore of baseline EAT as an independent predictive factor to stratify LVMI regression after TAVR. The Radscore has been incorporated into a clinically relevant nomogram model, which can accurately predict the probability of inadequate LVMI regression. Our radiomics nomogram has demonstrated that patients with a lower Radscore before TAVR are more likely to experience inadequate LVMI regression one year after TAVR. This information can assist clinicians in effectively managing LV remodeling in patients undergoing TAVR.

EAT has been extensively reported to be correlated with LV mass in individuals with normal, ischemic, and hypertrophic hearts.[20–22] According to previous hypotheses, the pathophysiology of EAT-induced LV hypertrophy may involve two distinct aspects.[23] Firstly, larger EAT, which reflects central obesity and increased visceral adipose tissue volume, may lead to greater energy requirements and increased ventricular workload, thereby promoting cardiac remodeling. Secondly, abundant evidence have shown that EAT is a metabolically active organ that produces various pro- and anti-inflammatory mediators and cytokines.[24] Inflammatory markers such as tumour necrosis factor-α, leptin, resistin and interleukin-6 and interleukin-17, secreting from EAT in response to injurious stimuli, might contribute to the pathogenesis of LV remodeling.[23,25] These findings collectively suggest that EAT may participate in the process of LV remodeling and regression through both quantitative and metabolic mechanisms.

Arangalage, *et al.*[10] discovered a significant correlation between the volume of EAT and LV mass in patients with asymptomatic degenerative AS. Furthermore, Yang, *et al.*[6] observed that a decrease in LVMI was associated with an increase in EAT volume and a decrease in average CT attenuation one year after TAVR. These findings support the hypothesis that the quantity of EAT may be linked to LV remodeling and regression. Additionally, Mancio, *et al.*[11] demonstrated EAT radiomics texture of patients with new-onset AF after aortic valve replacement was heterogeneous and exhibited higher maximum attenuation values than sinus rhythm patients, which correlated with up-regulation of inflammatory and down-regulation of lipid droplet-formation EAT

Table 2 Comparison of the three radiomics feature classifiers.

	Random forest		Logistic regression		Support vector machine	
	Training cohort	Validation cohort	Training cohort	Validation cohort	Training cohort	Validation cohort
AUC	1.00	0.69	0.77	0.74	0.87	0.74
Sensitivity	1.00	0.56	0.30	0.44	0.24	0.22
Specificity	1.00	0.89	0.90	1.00	1.00	0.95
Accuracy	1.00	0.79	0.73	0.82	0.78	0.71
F1 score	1.00	0.63	0.39	0.62	0.39	0.33

AUC: area under the curve.

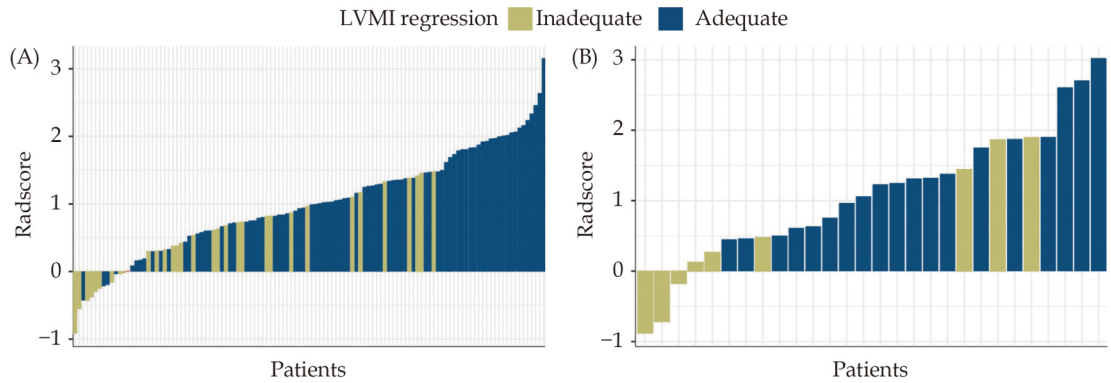

Figure 3 The histogram of Radscore for each patient in the training cohort (A) and validation cohort (B). LVMI: left ventricular mass index.

Table 3 The results of logistic regression.

Variable	Univariate logistic regression		Multivariable logistic regression	
	OR (95% CI)	*P*-value	OR (95% CI)	*P*-value
Age	1.048 (0.988–1.114)	0.13	1.039 (0.973–1.113)	0.26
Male	0.834 (0.405–1.724)	0.62	0.908 (0.383–2.159)	0.83
Body mass index	0.996 (0.890–1.111)	0.94	0.971 (0.853–1.102)	0.66
Diabetes mellitus	1.562 (0.631–3.729)	0.32	NA	NA
Hypertension	1.098 (0.522–2.281)	0.80	NA	NA
Atrial fibrillation	2.230 (0.903–5.431)	0.08	1.624 (0.584–4.443)	0.35
Aortic regurgitation > mild	0.503 (0.240–1.051)	0.07	0.698 (0.290–1.702)	0.42
Mean pressure gradient of trans–aortic blood flow	0.980 (0.959–0.999)	0.046	0.988 (0.965–1.009)	0.28
Radscore	0.226 (0.115–0.407)	< 0.001	0.262 (0.128–0.492)	< 0.001

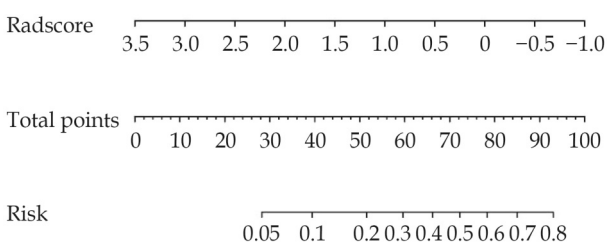

Figure 4 The radiomics nomogram for LVMI regression mode stratification of TAVR patients. LVMI: left ventricular mass index; TAVR: transcatheter aortic valve replacement.

proteins. This suggests that the radiomics analysis of EAT can provide insights into the metabolic status that directly affects the heart. Radiomics encompasses all data obtained from medical image, including the analysis of original imaging, application of filters, and mathematical transformations. It enables the quantitative description of (1) the distribution of attenuation (grey-level) values (first-order features); (2) spatial relations, heterogeneity, and coarseness of attenuation (textural features or second-order features); and (3) geometric properties (size/shape features). Thus, radiomics features from EAT can assess both the quantity of EAT, indicating the approximate amount of energy demand based on size/shape features, and the metabolism of EAT, indicating adipose content characteristics through the analysis of attenuation values. In our results, both geometric properties (including original-shape-maximum 2D diameter column) and spatial relations, heterogeneity, and coarseness of attenuation (log sigma 1 mm 3D-GLDM-dependence nonuniformity, log sigma 3 mm 3D-NGTDM-coarseness, wavelet HLL-firstorder-kurtosis, wavelet HLH-GLCM-correlation, wavelet HLL-GLRLM-gray level variance) from baseline EAT radiomics were found to be significantly associated with different LVMI regression modes up to one year after TAVR. This further validates the two aspects of the pathophysiology mechanism of LV hypertrophy influenced by EAT. Due to the absence of fascia-like structures separating it from the myocardium, EAT is likely to directly interact with the underlying myocardium and strongly contribute to LV mass regression, surpassing other factors such as BMI and hypertension. This could also explain our failure in selecting significant clinical

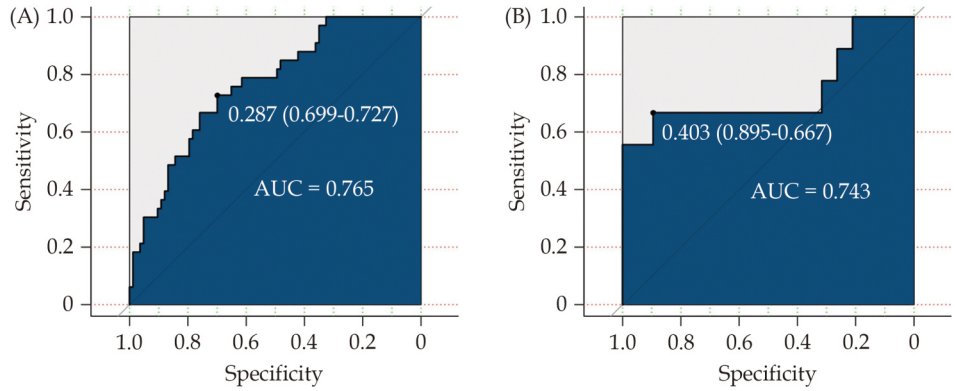

Figure 5 The receiver operating characteristic curves of the radiomics nomogram for the training cohort (A) and validation cohort (B). AUC: area under the curve.

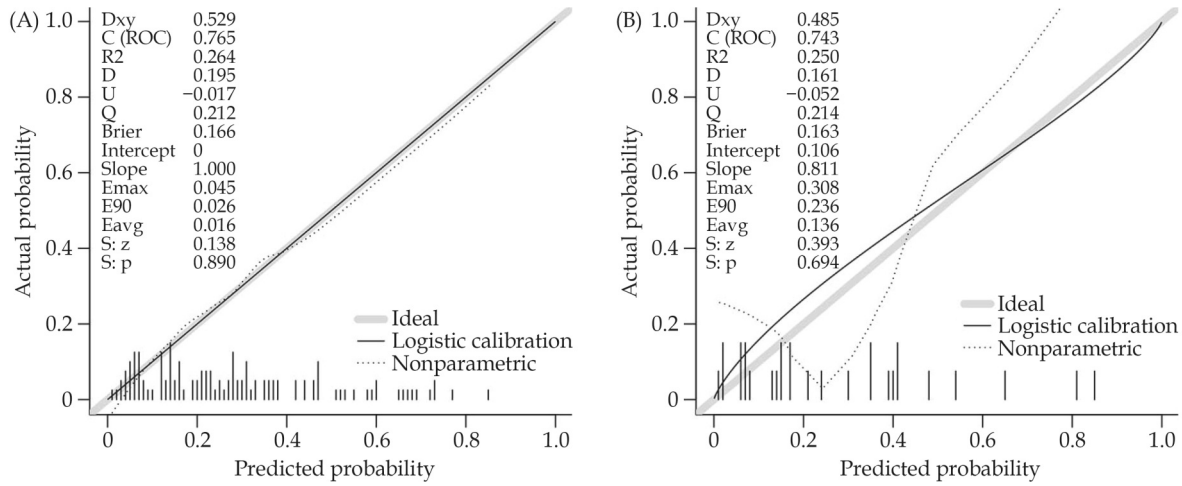

Figure 6 The calibration curves of the radiomics nomogram (logistic calibration) for the training cohort (A) and validation cohort (B).

predictors of inadequate LVMI regression in our multivariable analysis with EAT Radscore.

The nomogram in our study, serving as a predictive tool, integrates the independent predictive factor: Radscore and visualizes its overall impact on LVMI regression in each patient, aiding clinicians in developing management plans.[26] Nomograms have been widely used in diagnostic or prognostic studies of tumors due to their convenience and accuracy.[27–29] Their strong robustness has been confirmed in studies combining radiomics features and traditional clinical features to construct a nomogram.[30,31] Our results present the first nomogram in the TAVR population, allowing for better prediction of inadequate LVMI regression, with favorable outcomes validated by an independent validation cohort and decision curve analysis of clinical benefit. This tool from readily available CT imaging identifies high-risk patients of inadequate LVMI regression, thus makes it possible to early intervene the risk after TAVR by considering the administration of medications that improve LV remodeling or regulate cytokines secreted by EAT (e.g., statins[32]). As the TAVR indication has now expanded to surgically low-risk patients who are significantly younger,[33] the benefit of early identification and intervention of predicted worse LV response may be greater.

LIMITATIONS

However, our study has several limitations that should be acknowledged. Firstly, it is important to note that this study was conducted at a single center and had a relatively small sample size. While we have independently validated the model, it is crucial to obtain additional evidence from multi-center studies to independently validate the robustness and repeatability of the nomogram. Secondly, although the combination method of the *t*-test and LASSO regression yielded efficient outcomes, it may not be the most stable approach for se-

lecting radiomic features. Therefore, it is recommended that future research explores alternative feature selection methods. Last but not least, due to a lack of available data, we were unable to include inflammative or metabolic parameters to further investigate the relationship between metabolism and CT radiomics performance of EAT. This area requires further investigation.

CONCLUSIONS

In conclusion, our research has successfully developed and validated a radiomics nomogram based on preprocedural CT imaging. This nomogram serves as a valuable tool for clinicians in making better stratification and management decisions regarding inadequate LVMI regression in the context of TAVR. The underlying mechanism of EAT involvement in LV mass regression after TAVR, as well as the presented efficient prediction tool, the radiomics nomogram, based on a limited number of patients, warrant further investigation.

ACKNOWLEDGMENTS

This study was supported by the National Natural Science Foundation of China (No.82170375 & No.8210 2129 & U23A20395), the 1·3·5 Project for Disciplines of Excellence from West China Hospital of Sichuan University (ZYGD23021), and the Sichuan Science and Technology Program (No.2024NSFSC1714 & No.2024 NSFSC1716). All authors had no conflicts of interest to disclose.

REFERENCES

[1] Cioffi G, Faggiano P, Vizzardi E, *et al*. Prognostic effect of inappropriately high left ventricular mass in asymptomatic severe aortic stenosis. *Heart* 2011; 97: 301–307.
[2] Levy D, Garrison RJ, Savage DD, *et al*. Prognostic implications of echocardiographically determined left ventricular mass in the Framingham Heart Study. *N Engl J Med* 1990; 322: 1561–1566.
[3] Mihaljevic T, Nowicki ER, Rajeswaran J, *et al*. Survival after valve replacement for aortic stenosis: implications for decision making. *J Thorac Cardiovasc Surg* 2008; 135: 1270–1278.
[4] Chau KH, Douglas PS, Pibarot P, *et al*. Regression of left ventricular mass after transcatheter aortic valve replacement: the PARTNER trials and registries. *J Am Coll Cardiol* 2020; 75: 2446–2458.
[5] Chen SC, Leu HB, Chang HH, *et al*. Women had favourable reverse left ventricle remodelling after TAVR. *Eur J Clin Invest* 2020; 50: e13183.
[6] Yang HR, Xiong TY, Zhang Y, *et al*. Concomitant aortic regurgitation predicts better left ventricular reverse remodeling after transcatheter aortic valve replacement. *BMC Cardiovasc Disord* 2023; 23: 354.
[7] Dobson LE, Musa TA, Uddin A, *et al*. The impact of transcatheter aortic valve replacement induced left-bundle branch block on cardiac reverse remodeling. *J Cardiovasc Magn Reson* 2017; 19: 22.
[8] Davin L, Nchimi A, Ilardi F, *et al*. Epicardial adipose tissue and myocardial fibrosis in aortic stenosis relationship with symptoms and outcomes: a study using cardiac magnetic resonance imaging. *JACC Cardiovasc Imaging* 2019; 12: 213–214.
[9] Eberhard M, Stocker D, Meyer M, *et al*. Epicardial adipose tissue volume is associated with adverse outcomes after transcatheter aortic valve replacement. *Int J Cardiol* 2019; 286: 29–35.
[10] Arangalage D, Mathieu T, Nguyen V, *et al*. Epicardial adipose tissue volume is associated with left ventricular remodelling in calcific aortic valve stenosis. *Arch Cardiovasc Dis* 2019; 112: 594–603.
[11] Mancio J, Sousa-Nunes F, Martins R, *et al*. Decoding the radiomic and proteomic phenotype of epicardial adipose tissue associated with adverse left atrial remodelling and post-operative atrial fibrillation in aortic stenosis. *Eur Heart J Cardiovasc Imaging* 2022; 23: 1248–1259.
[12] Ponsiglione A, Stanzione A, Cuocolo R, *et al*. Cardiac CT and MRI radiomics: systematic review of the literature and radiomics quality score assessment. *Eur Radiol* 2022; 32: 2629–2638.
[13] Jia X, Zhai Y, Song D, *et al*. A multiparametric MRI-based radiomics nomogram for preoperative prediction of survival stratification in glioblastoma patients with standard treatment. *Front Oncol* 2022; 12: 758622.
[14] Lang RM, Badano LP, Mor-Avi V, *et al*. Recommendations for cardiac chamber quantification by echocardiography in adults: an update from the American Society of Echocardiography and the European Association of Cardiovascular Imaging. *J Am Soc Echocardiogr* 2015; 28: 1-39. e14.
[15] Nappi C, Ponsiglione A, Acampa W, *et al*. Relationship between epicardial adipose tissue and coronary vascular function in patients with suspected coronary artery disease and normal myocardial perfusion imaging. *Eur Heart J Cardiovasc Imaging* 2019; 20: 1379–1387.
[16] Fedorov A, Beichel R, Kalpathy-Cramer J, *et al*. 3D Slicer as an image computing platform for the Quantitative Imaging Network. *Magn Reson Imaging* 2012; 30: 1323–1341.
[17] van Griethuysen JJM, Fedorov A, Parmar C, *et al*. Computational radiomics system to decode the radiographic phenotype. *Cancer Res* 2017; 77: e104–e107.
[18] Balachandran VP, Gonen M, Smith JJ, *et al*. Nomograms in oncology: more than meets the eye. *Lancet Oncol* 2015; 16: e173–e180.
[19] Nguyễn MV, Carlier C, Nich C, *et al*. Fracture risk of long bone metastases: a review of current and new decision-making tools for prophylactic surgery. *Cancers (Basel)* 2021; 13: 3662.
[20] Bakkum MJ, Danad I, Romijn MA, *et al*. The impact of obesity on the relationship between epicardial adipose tissue, left ventricular mass and coronary microvascular function. *Eur J Nucl Med Mol Imaging* 2015; 42: 1562–1573.

[21] Iacobellis G, Ribaudo MC, Zappaterreno A, *et al*. Relation between epicardial adipose tissue and left ventricular mass. *Am J Cardiol* 2004; 94: 1084–1087.
[22] Corradi D, Maestri R, Callegari S, *et al*. The ventricular epicardial fat is related to the myocardial mass in normal, ischemic and hypertrophic hearts. *Cardiovasc Pathol* 2004; 13: 313–316.
[23] de Simone G, Izzo R, De Luca N, *et al*. Left ventricular geometry in obesity: is it what we expect? *Nutr Metab Cardiovasc Dis* 2013; 23: 905-912.
[24] Mazurek T, Zhang L, Zalewski A, *et al*. Human epicardial adipose tissue is a source of inflammatory mediators. *Circulation* 2003; 108: 2460–2466.
[25] Iacobellis G, Corradi D, Sharma AM. Epicardial adipose tissue: anatomic, biomolecular and clinical relationship with the heart. *Nat Clin Pract Cardiovasc Med* 2005; 2: 536–543.
[26] Kattan MW. Nomograms. *Introduction. Semin Urol Oncol* 2002; 20: 79–81.
[27] Yang L, Dong D, Fang M, *et al*. Can CT-based radiomics signature predict KRAS/NRAS/BRAF mutations in colorectal cancer? *Eur Radiol* 2018; 28: 2058-2067.
[28] Xie T, Wang X, Li M, *et al*. Pancreatic ductal adenocarcinoma: a radiomics nomogram outperforms clinical model and TNM staging for survival estimation after curative resection. *Eur Radiol* 2020; 30: 2513–2524.
[29] Zhang W, Fang M, Dong D, *et al*. Development and validation of a CT-based radiomic nomogram for preoperative prediction of early recurrence in advanced gastric cancer. *Radiother Oncol* 2020; 145: 13–20.
[30] Zhang X, Lu H, Tian Q, *et al*. A radiomics nomogram based on multiparametric MRI might stratify glioblastoma patients according to survival. *Eur Radiol* 2019; 29: 5528–5538.
[31] Huang YQ, Liang CH, He L, *et al*. Development and validation of a radiomics nomogram for preoperative prediction of lymph node metastasis in colorectal cancer. *J Clin Oncol* 2016; 34: 2157–2164.
[32] Parisi V, Petraglia L, D'Esposito V, *et al*. Statin therapy modulates thickness and inflammatory profile of human epicardial adipose tissue. *Int J Cardiol* 2019; 274: 326–330.
[33] Quarta S, Santarpino G, Carluccio MA, *et al*. Exploring the significance of epicardial adipose tissue in aortic valve stenosis and left ventricular remodeling: unveiling novel therapeutic and prognostic markers of disease. *Vascul Pharmacol* 2023; 152: 107210.

Please cite this article as: ZHANG Y, YANG HR, JI XY, XIONG TY, CHEN M. Radiomics of baseline epicardial adipose tissue predicts left ventricular mass regression after transcatheter aortic valve replacement. *J Geriatr Cardiol* 2024; 21(12): 1109–1118. DOI: 10.26599/1671-5411.2024.12.005